Chapter 2

Statistical analysis of MHD convective ferro-nanofluid flow through an inclined channel with Hall current *

2.1 Introduction

Molecule transport in a slanted rectangular channel is usual in designing applications, e.g. molecule transport in micro channels. Slanted pipe and channels have extensive applications in automobile industry for designing equipments. Nanoparticles can considerably reduce the size of equipments and show a better performance than the existing ones. Convection flow through the vertical channel is decisive in the cooling system of heat exchangers and solar cells. Warm blood circulation in mammals and engine cooling are examples of convection. Forced and free convections are very important in the convection flows. Chemical reaction and radiation impacts on MHD convective nanofluid flow through an inclined channel with Hall current, heat source and Soret effect are analyzed using ferro-nanofluid. In addition, the resultant thermal conductivity is found using the Hamilton-Crosser model. Besides, wall heat, mass transfer rates and surface drag are investigated through statistical tools like regression and probable error.

2.2 Mathematical formulation

An unsteady free convective, incompressible and electrically conducting ferro-nanofluid flow through an inclined channel packed with porous medium is considered. The problem is studied under the following assumptions:

*Published in: Thermal Science and Engineering Progress (Elsevier), 2021; 22; 100816

1. Ferro-nanofluid flow is observed in the X^* direction.
2. Two infinite electrically non-conducting and permeable parallel plates at a distance d apart inclined at an angle α are considered (see Fig. 2.1).
3. One plate is held stationary while the other is oscillating in its own plane with a velocity $U^*(t^*)$.
4. Ferro-nanofluid is injected into the stationary plate with a velocity w_0 and is sucked by the oscillating plate with a velocity w_0.
5. A uniform magnetic field of strength B_0 is exerted in the Z^* axis (orthogonal to the flow) and Hall current is generated due to this magnetic field.
6. Effect of induced electric and magnetic field are ignored due to small magnetic Reynolds number.
7. Temperature and concentration at the stationary plate periodically varies with time t^*.
8. Plates are maintained at high-temperature variation to induce heat transfer via radiation. The radiative heat flux is considered in the Z^* direction.
9. Density variation with temperature and concentration in body force term is considered and all other fluid properties are assumed to be constant.
10. Additional heat source (Q) and the order of reactive species in an irreversible chemical reaction are considered.
11. Viscous dissipation, Joule heating, electric and polarisation effects are ignored (Balvinder, Krishan, & Bansal, 2014).

Using Boussinesq's approximation, the flow is described (Singh & Mathew, 2012), (Pal & Talukdar, 2013), (Sureshkumar & Muthtamilselvan, 2016)as:

$$\begin{aligned}\rho_{nf}\left(\tfrac{\partial u^*}{\partial t^*}+w_0\tfrac{\partial u^*}{\partial z^*}\right) &= -\tfrac{\partial P}{\partial x^*}+\mu_{nf}\tfrac{\partial^2 u^*}{\partial z^{*2}} \ +(\rho\beta_T)_{nf}g\,(T^*-T_d)\,sin\alpha \\ &+(\rho\beta_C)_{nf}g\,(C^*-C_d)\sin\alpha \ +\tfrac{\sigma {B_0}^2(Hv^*-u^*)}{1+H^2}-\tfrac{\mu_{nf}}{K_p}u^*\end{aligned} \tag{2.2.1}$$

$$\rho_{nf}\left(\frac{\partial v^*}{\partial t^*}+w_0\frac{\partial v^*}{\partial z^*}\right)=-\frac{\partial P}{\partial y^*}+\mu_{nf}\frac{\partial^2 v^*}{\partial z^{*2}}-\frac{\sigma {B_0}^2\,(Hu^*+v^*)}{1+H^2}-\frac{\mu_{nf}}{K_p}v^* \tag{2.2.2}$$

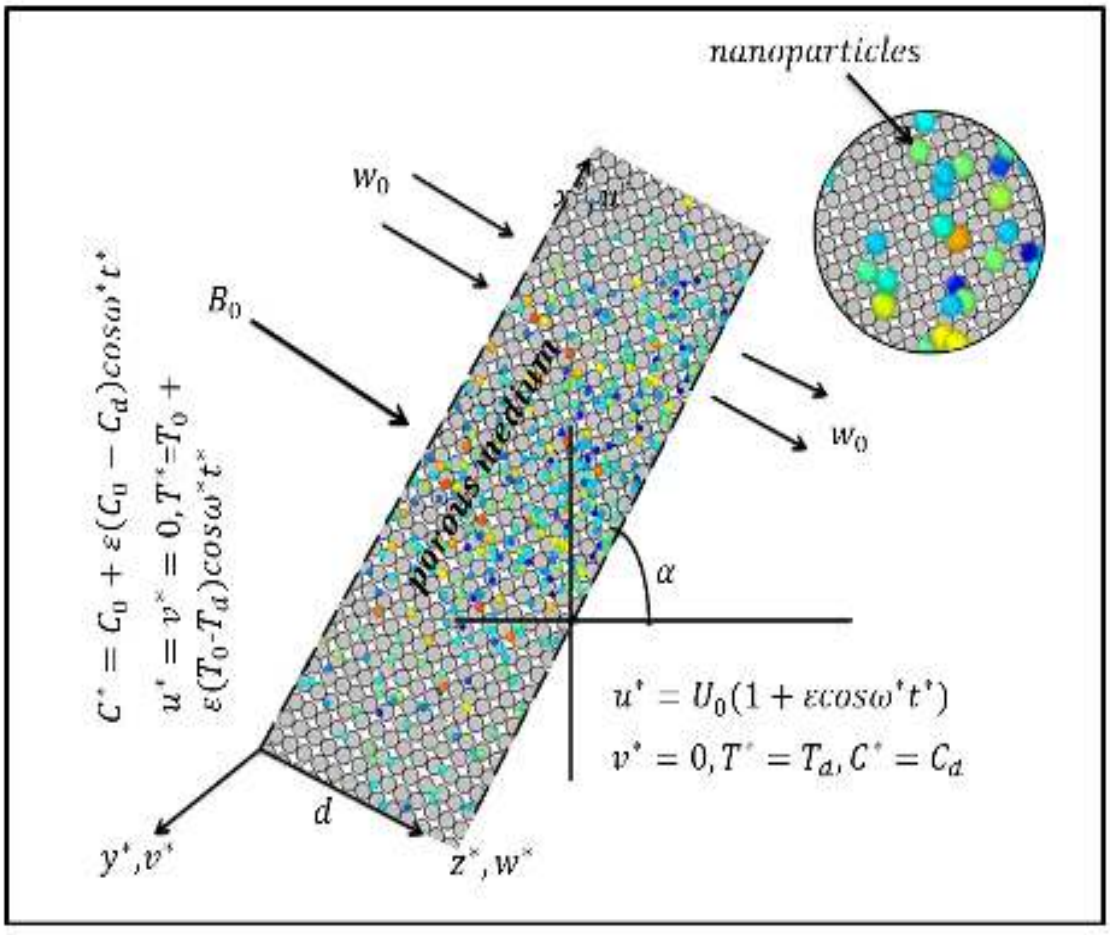

Figure 2.1: *Physical configuration of the problem*

$$(\rho C_p)_{nf}\left(\frac{\partial T^*}{\partial t^*} + w_0\frac{\partial T^*}{\partial z^*}\right) = k_{nf}\frac{\partial^2 T^*}{\partial z^{*2}} - \frac{\partial q_R}{\partial z^*} + Q\,(T^* - T_d) \tag{2.2.3}$$

$$\frac{\partial C^*}{\partial t^*} + w_0\frac{\partial C^*}{\partial z^*} = D_B\frac{\partial^2 C^*}{\partial z^{*2}} + D_T\frac{\partial^2 T^*}{\partial z^{*2}} - K_l\,(C^* - C_d) \tag{2.2.4}$$

where the terms are explained in nomenclature.

Optically thin nanofluid has been considered and hence radiative heat flux (Balvinder et al., 2014) is taken as

$$\frac{\partial q_R}{\partial z^*} = 4{\alpha_P}^2\,(T_0 - T_d) \tag{2.2.5}$$

Corresponding boundary conditions are:

$$\left.\begin{array}{c} u^* = v^* = 0,\ T^* = T_0 + \epsilon\,(T_0 - T_d)\,cos\omega^* t^*,\ C^* = C_0 + \epsilon\,(C_0 - C_d)\,cos\omega^* t^*,\ z^* = 0 \\ u^* = U_0\,(1 + \epsilon cos\omega^* t^*)\,,\quad v^* = 0,\quad T^* = T_d,\ C^* = C_d,\quad z^* = d \end{array}\right\} \tag{2.2.6}$$

Following quantities are used to make equations (2.2.1) to (2.2.4) in dimensionless form:

$$\begin{gathered} K_r = \frac{K_l \nu}{{w_0}^2}, D_B = \frac{\nu}{Sc},\ R = \frac{2\alpha_P d}{\sqrt{K}},\ Re = \frac{U_0 d}{\nu},\ \lambda = \frac{w_0 d}{\nu}, M = B_0 d\sqrt{\frac{\sigma}{\mu}}, \\ z = \frac{z^*}{d},\ x = \frac{x^*}{d}, t = t^*\omega^*, u = \frac{u^*}{U_0}, v = \frac{v^*}{U_0}\ , \omega = \frac{\omega^* d^2}{\nu}, \\ U = \frac{U^*}{U_0}, K_1 = \frac{K_p}{d^2},\ S = \frac{Qd^2}{K}, Pr = \frac{\mu C_p}{K}, G_m\ = \frac{\nu g\beta(C_0 - C_d)}{U_0 {w_0}^2} \\ S_0 = \frac{D_T(T_0 - T_d)}{(C_0 - C_d)\nu}, \theta' = \frac{T^* - T_d}{(T_0 - T_d)}, C' = \frac{C^* - C_d}{(C_0 - C_d)}, G_r = \frac{\nu g\beta(T_0 - T_d)}{U_0 {w_0}^2} \end{gathered} \tag{2.2.7}$$

The nanofluid constants are stated (O. Makinde & Animasaun, 2016) as follows:

$$\begin{gathered} \rho_{nf} = (1-\phi)\,\rho_f + \phi\rho_s, \mu_{nf} = \frac{\mu_f}{(1-\phi)^{2.5}}, \\ (\rho C_p)_{nf} = (1-\phi)\,(\rho C_p)_f + \phi(\rho C_p)_s, \\ \lambda_n = \frac{k_{nf}}{k_f} = \frac{k_s + (h-1)k_f - (h-1)\left(k_f - k_s\right)\phi}{k_s + (h-1)k_f + \left(k_f - k_s\right)\phi}, \\ \frac{\sigma_{nf}}{\sigma_f} = 1 + \frac{3\left(\frac{\sigma_s}{\sigma_f} - 1\right)\phi}{\frac{\sigma_s}{\sigma_f} - 2 - \left(\frac{\sigma_s}{\sigma_f} - 1\right)\phi}, \\ (\rho\beta_T)_{nf} = (1-\phi)\,(\rho\beta_T)_f + \phi(\rho\beta_T)_s, \end{gathered} \tag{2.2.8}$$

Let $\beta_T = \beta_C$ and assume that

$$\begin{gathered} \phi_1 = 1 - \phi + \phi\frac{\rho_s}{\rho_f},\ \phi_2 = \frac{1}{(1-\phi)^{2.5}}, \\ \phi_3 = 1 - \phi + \phi\frac{(\rho\beta_T)_s}{(\rho\beta_T)_f}, \\ \phi_4 = 1 - \phi + \phi\frac{(\rho C_p)_s}{(\rho C_p)_f}, \\ \phi_5 = \frac{\sigma_{nf}}{\sigma_f}, \end{gathered} \tag{2.2.9}$$

Let $l' = u + iv$ and $h = 3$, then the equations (2.2.1) to (2.2.4) along with condition

Table 2.1: *Thermo physical properties of base fluid and nanoparticles at* 25^0

Model	$\rho\,(kgm^{-3})$	$C_p\,(Jkg^{-1}K^{-1})$	$k\,(Wm^{-1}K^{-1})$	$\beta \times 10^{-5}\,(K^{-1})$	$\sigma\,(s/m)$
Water	997.1	4179	0.613	21	0.05
Fe_3O_4	5180	670	9.7	1.3	25000

(2.2.6) are transformed into the non-dimensional form given by:

$$\begin{aligned}\phi_1\left(\omega\frac{\partial l'}{\partial t}+\lambda\frac{\partial l'}{\partial z}\right)=\phi_1\omega\frac{\partial U}{\partial t}+\phi_2\frac{\partial^2 l'}{\partial z^2}+\phi_3\lambda^2 sin\alpha\,(Gr\;\theta'+Gm\;C')\\-(l'-U)\left(\frac{\phi_2}{K_1}+\frac{\phi_5 M^2}{1+H^2}\,(1+iH)\right)\end{aligned}\tag{2.2.10}$$

$$\phi_4\left(\omega\frac{\partial\theta'}{\partial t}+\lambda\frac{\partial\theta'}{\partial z}\right)=\frac{1}{Pr}\left(\lambda_n\frac{\partial^2\theta'}{\partial z^2}-R^2\theta'+S\theta'\right)\tag{2.2.11}$$

$$\omega\frac{\partial C'}{\partial t}+\lambda\frac{\partial C'}{\partial z}=\frac{1}{Sc}\frac{\partial^2 C'}{\partial z^2}+S_0\frac{\partial^2\theta'}{\partial z^2}-K_r\lambda^2 C'\tag{2.2.12}$$

The corresponding boundary conditions are:

$$\left.\begin{aligned}l'=0,\quad \theta'=C'=1+\epsilon cost,\quad z=0\\ l'=1+\epsilon cost,\quad \theta'=0,\quad C'=0,\quad z=1\end{aligned}\right\}\tag{2.2.13}$$

2.3 Numerical solution

Solutions of equation (2.2.10) to (2.2.13) are approximated (Telionis & Telionis, 1981) as:

$$\delta'=\delta'_0(z)+\frac{\epsilon}{2}\left(\delta'_1(z)\,e^{(it)}+\delta'_2(z)\,e^{(-it)}\right)\tag{2.3.1}$$

Replacing δ' by the terms l', θ' and C' and applying in equations (2.2.10)-(2.2.13) we have:

$$\theta'_0=m_1e^{(\eta_1 z)}+m_2e^{(\eta_2 z)}\tag{2.3.2}$$

$$\theta'_1=m_3e^{(\eta_3 z)}+m_4e^{(\eta_4 z)}\tag{2.3.3}$$

$$\theta'_2=m_5e^{(\eta_5 z)}+m_6e^{(\eta_6 z)}\tag{2.3.4}$$

$$C'_0=\zeta_1e^{(q_1 z)}+\zeta_2e^{(q_2 z)}+A_{11}e^{(\eta_1 z)}+A_{12}e^{(\eta_2 z)}\tag{2.3.5}$$

$$C'_1=\zeta_3e^{(q_3 z)}+\zeta_4e^{(q_4 z)}+A_{21}e^{(\eta_3 z)}+A_{22}e^{(\eta_4 z)}\tag{2.3.6}$$

$$C'_2=\zeta_5e^{(q_5 z)}+\zeta_6e^{(q_6 z)}+A_{31}e^{(\eta_5 z)}+A_{32}e^{(\eta_6 z)}\tag{2.3.7}$$

$$\begin{aligned}l'_0=h_1e^{(\chi_1 z)}+h_2e^{(\chi_2 z)}+D_{11}+D_{12}e^{(\eta_1 z)}+D_{13}e^{(\eta_2 z)}\\+D_{14}e^{(q_1 z)}+D_{15}e^{(q_2 z)}+D_{16}e^{(\eta_1 z)}+D_{17}e^{(\eta_2 z)}\end{aligned}\tag{2.3.8}$$

$$\begin{aligned}l'_1=h_3e^{(\chi_3 z)}+h_4e^{(\chi_4 z)}+D_{21}+D_{22}e^{(\eta_3 z)}+D_{23}e^{(\eta_4 z)}\\+D_{24}e^{(q_3 z)}+D_{25}e^{(q_4 z)}+D_{26}e^{(\eta_3 z)}+D_{27}e^{(\eta_4 z)}\end{aligned}\tag{2.3.9}$$

$$\begin{aligned} l'_2 = h_5 e^{(\chi_5 z)} + h_6 e^{(\chi_6 z)} + D_{31} + D_{32} e^{(\eta_5 z)} + D_{33} e^{(\eta_6 z)} \\ + D_{34} e^{(q_5 z)} + D_{35} e^{(q_6 z)} + D_{36} e^{(\eta_5 z)} + D_{37} e^{(\eta_6 z)} \end{aligned} \tag{2.3.10}$$

$$\left.\begin{array}{c} \text{Local Nusselt number } Nu = \frac{x^* q_w}{K_f(T_0 - T_d)} \\ \text{local Sherwood number } \ Sh = \frac{x^* q_m}{D_B(C_0 - C_d)} \\ \text{Skin friction coefficient } \ Cf = \frac{\tau_w}{\rho_f U_0^2} \end{array}\right\} \tag{2.3.11}$$

where

$$q_w = -k_{nf}\frac{\partial T^*}{\partial z^*}, \quad q_m = -D_B\frac{\partial C^*}{\partial z^*}, \quad \tau_w = \mu_{nf}\frac{\partial u^*}{\partial z^*} \tag{2.3.12}$$

Using the non-dimensional quantities (2.2.7), the above expressions are transformed into:

$$Nu = -\lambda_n\frac{\partial \theta'}{\partial z}, \quad Sh = -\frac{\partial C'}{\partial z}, \qquad Cf = \frac{\phi_2}{Re}\frac{\partial l'}{\partial z} \tag{2.3.13}$$

Nusselt Number Nu at z = 1

$$Nu = -\lambda_n\left(\frac{\partial \theta'}{\partial z}\right)_{z=1} \tag{2.3.14}$$

$$Nu = -\lambda_n\left(Nu_0 + \frac{\varepsilon}{2}\left(Nu_1 e^{(it)} + Nu_2 \mathrm{e}^{(-\mathrm{it})}\right)\right) \tag{2.3.15}$$

where

$$Nu_0 = \eta_1 m_1 \mathrm{e}^{(\eta_1)} + \eta_2 m_2 \mathrm{e}^{(\eta_2)} \tag{2.3.16}$$

$$Nu_1 = \eta_3 m_3 \mathrm{e}^{(\eta_3)} + \eta_4 m_4 \mathrm{e}^{(\eta_4)} \tag{2.3.17}$$

$$Nu_2 = \eta_5 m_5 \mathrm{e}^{(\eta_5)} + \eta_6 m_6 \mathrm{e}^{(\eta_6)} \tag{2.3.18}$$

Sherwood Number Sh at $z = 1$

$$Sh = -\left(\frac{\partial C'}{\partial z}\right)_{z=1} \tag{2.3.19}$$

$$Sh = -\left(Sh_0 + \frac{\varepsilon}{2}\left(Sh_1 e^{(it)} + Sh_2 \mathrm{e}^{(-\mathrm{it})}\right)\right) \tag{2.3.20}$$

where

$$Sh_0 = q_1\zeta_1 \mathrm{e}^{(\mathrm{q}_1)} + q_2\zeta_2 \mathrm{e}^{(\mathrm{q}_2)} + \eta_1 A_{11} e^{(\eta_1)} + \eta_2 A_{12} \mathrm{e}^{(\eta_2)} \tag{2.3.21}$$

$$Sh_1 = q_3\zeta_3 \mathrm{e}^{(\mathrm{q}_3)} + q_4\zeta_4 \mathrm{e}^{(\mathrm{q}_4)} + \eta_3 A_{21} \mathrm{e}^{(\eta_3)} + \eta_4 A_{22} \mathrm{e}^{(\eta_4)} \tag{2.3.22}$$

$$Sh_2 = q_5\zeta_5 \mathrm{e}^{(\mathrm{q}_5)} + q_6\zeta_6 \mathrm{e}^{(\mathrm{q}_6)} + \eta_5 A_{31} \mathrm{e}^{(\eta_5)} + \eta_6 A_{32} \mathrm{e}^{(\eta_6)} \tag{2.3.23}$$

Skin friction Coefficient C_f at $z = 1$

$$Cf = \frac{\phi_2}{Re}\left(\frac{\partial l'}{\partial z}\right)_{z=1} \tag{2.3.24}$$

$$Cf = \frac{\phi_2}{Re}\left(Cf_0 + \frac{\varepsilon}{2}\left(Cf_1 e^{(it)} + Cf_2 e^{(-it)}\right)\right) \tag{2.3.25}$$

where

$$\begin{gathered} Cf_0 = \chi_1 h_1 e^{(\chi_1)} + \chi_2 h_2 e^{(\chi_2)} \quad + \eta_1 D_{12}\mathrm{e}^{(\eta_1)} + \eta_2 D_{13} e^{(\eta_2)} + \\ q_1 D_{14} e^{(q_1)} + q_2\ D_{15}\mathrm{e}^{(\mathrm{q}_2)} + \eta_1 D_{16}\mathrm{e}^{(\eta_1)} + \eta_2 D_{17}\mathrm{e}^{(\eta_2)} \end{gathered} \tag{2.3.26}$$

$$\begin{gathered} Cf_1 = \chi_3 h_3 e^{(\chi_3)} + \chi_4 h_4 \mathrm{e}^{(\chi_4)} \\ + \eta_3 D_{22}\mathrm{e}^{(\eta_3)} + \eta_4 D_{23}\mathrm{e}^{(\eta_4)} + q_3 D_{24}\mathrm{e}^{(\mathrm{q}_3)} + q_4 D_{25}\mathrm{e}^{(\mathrm{q}_4)} + \eta_3 D_{26}\mathrm{e}^{(\eta_3)} + \eta_4 D_{27}\mathrm{e}^{(\eta_4)} \end{gathered} \tag{2.3.27}$$

$$\begin{gathered} Cf_2 = \chi_5 h_5 \mathrm{e}^{(\chi_5)} + \chi_6 h_6 \mathrm{e}^{(\chi_6)} + \eta_5 D_{32}\mathrm{e}^{(\eta_5)} + \eta_6 D_{33}\mathrm{e}^{(\eta_6)} + q_5\ D_{34}\mathrm{e}^{(\mathrm{q}_5)} \\ + q_6 D_{35}\mathrm{e}^{(\mathrm{q}_6)} + \eta_5 D_{36}\mathrm{e}^{(\eta_5)} + \eta_6 D_{37}\mathrm{e}^{(\eta_6)} \end{gathered} \tag{2.3.28}$$

The amplitude (τ_{0r}) and phase difference (β_0) of shear stress at $z = 0$ in the case of steady flow is defined as $\tau_{0r} = \sqrt{\tau_{0x}^2 + \tau_{0y}^2}$ and $\beta_o = \tan^{-1}\left(\frac{\tau_{0y}}{\tau_{0x}}\right)$; where $\left(\frac{\partial l_0'}{\partial z}\right)_{z=0} = \tau_{0x} + i\tau_{0y}$,

$$\left(\frac{\partial l_0'}{\partial z}\right)_{z=0} = \chi_1 h_1 + \chi_2 h_2 \quad + \eta_1 D_{12} + \eta_2 D_{13} + D_{14} q_1 + D_{15} q_2 + D_{16}\eta_1 + D_{17}\eta_2. \tag{2.3.29}$$

The arbitrary constants appearing in the solutions are given in the appendix section. To validate the numerical values, comparison study has been carried out in Table 2.2 and Table 2.3 with previously published papers (P. K. Sharma, Sharma, & Chaudhary, 2007) and (Pal & Talukdar, 2013). The numerical values are found to be in excellent agreement.

2.4 Results and discussion

Fluid profiles for l', θ' and $C'$of ferro-nanofluid are plotted by choosing the following values:

$t = \frac{\pi}{4}, Pr = 6.07,\ \ G_r = 5,\ \ G_m = 5,\ \lambda = 1,\ R = 0.5,\ K_r = 1,\ K_1 = 0.7,\ M = 3,\ \ H = 0.5,\ S_0 = 1,\ S = 3,\ \omega = 10,\ Sc = 0.22,\ \phi = 0.04,\ h = 3,\ \alpha = 45^0,\ \ Re = 10,\ \epsilon = 0.01$

Table 2.2: *Amplitude value of the coefficient, $\frac{\varepsilon}{2}e^{it}$, in the expansion of $\left(\frac{\partial\theta'}{\partial z}\right)_{z=0}$ with $\lambda = 0, R = 0, S = 0, \phi = 0$.*

ω	(P. K. Sharma et al., 2007) $\left\|\left(\frac{\partial\theta_1}{\partial y}\right)_{y=0}\right\|$		Present Study $\left\|\left(\frac{\partial\theta_1'}{\partial z}\right)_{z=0}\right\|$	
	$Pr = 0.71$	$Pr = 7$	$Pr = 0.71$	$Pr = 7$
2	1.144	3.762	1.1438	3.7623
4	1.474	5.293	1.4745	5.2937
6	1.857	6.479	1.8575	6.4794
8	2.228	7.483	2.2289	7.4832
10	2.568	8.366	2.5668	8.3667

Table 2.3: *Comparison of (τ_{0r}) and (β_0) of the steady flow in the absence of Ω^*, with $G_m = 0, R = 0, K_r = 0, K_1 \to \infty, S_0 = 0, S = 0, \phi = 0, \alpha = \pi/2$.*

G_r	M	H	λ	Pr	(Pal & Talukdar, 2013)		Present Study	
					τ_{0r}	β_0	τ_{0r}	β_0
5	2	1	0.5	0.71	1.829935	0.265883	1.829935	0.265883
10	2	1	0.5	0.71	2.167691	0.20624	2.167692	0.20624
5	4	1	0.5	0.71	3.344788	0.370293	3.344789	0.370293
5	2	3	0.5	0.71	1.364854	0.255192	1.364854	0.255192
5	2	1	1	0.71	2.613122	0.142007	2.613122	0.142006
5	2	1	0.5	7	1.907705	0.246677	1.907705	0.246677

Thermophysical properties (Sheikholeslami & Ganji, 2014),(Kumar et al., 2018), (Aminfar, Mohammadpourfard, & Mohseni, 2012) of nanoparticles and base fluid at 25^0 are shown in the Table 2.1. Values of Cf, Nu and Sh are given in Tables 2.4-2.6. The effect of volume fraction and non-dimensional parameters has been studied using spherical shape Fe_3O_4 nano particles.

Figures 2.2 to 2.4 illustrate the impact of ϕ on l', θ' and C' profiles. It is understood from the plots that l' and θ'diminishes with increase in ϕ while concentration

increases. Figures 2.5 to 2.16 display the hold of diverse non-dimensional parameters on θ', l' and C' profiles. These profiles have been drawn according to the variation in z. The l' profile increases with rise in Hall current parameter (Figure 2.5) but velocity is diminishing with rise in M (Figure 2.6). The movement of ferro-nanofluid perpendicular to B_0 induces a Lorentz force against the fluid flow which retards the fluid velocity. Also, B_0 induces a Hall current which acts in the direction of the fluid flow and thus it accelerates the fluid velocity.

Concentration of ferro-nanofluid with variation in chemical reaction parameter is depicted in figures 2.7 and 2.8. The sign of chemical reaction parameter determines whether the chemical reaction is destructive or constructive (Sarma & Pandit, 2018). As $K_r(K_r > 0)$ increases, a destructive chemical reaction enhances and thus concentration of the nanofluid decreases. As K_r $(K_r < 0)$ decreases, a constructive chemical reaction enhances and hence concentration increases.

The profiles for l', θ' and C' of ferro-nanofluid with changes in heat source parameter are illustrated in the figures 2.9 to 2.11. A rise in S enhances the fluid temperature and increases the kinetic energy level in molecules of nanofluid. Consequently, l' of the ferro-nanofluid goes up and C' comes down.

l' *and* θ' profiles of the ferro-nanofluid with variation in injection/suction parameter are shown in figures 2.12 and 2.13. l' *and* θ' of the nanofluid near the oscillatory plate increases with increasing injection/suction parameter. As λ $(\lambda > 0)$ increases, heated fluid particles enter into the channel and cold fluid particles disappear from the channel increasing the velocity and temperature inside the channel. The process is reversed in the case λ $(\lambda < 0)$. Concentration profile of ferro- nanofluid with variation in Soret number is depicted in figure 2.14. Concentration decreases due to the increase in S_0. A step up in S_0 indicates the enhancement in $\theta^{'}$ difference and therefore C' is diminished. Figure 2.15 reveals that velocity of ferro-nanofluid increases with rise in α. This is due to the effect of increased gravitational force. Figure 2.16 depicts the level of enhancement in velocity profile with increasing porosity parameter.

Table 2.4: *The Skin friction of Fe_3O_4-water nanofluid when $t = \frac{\pi}{4}, Pr = 6.07, K_r = 1.5,\ K_1 = 0.7,\ \ M = 3.5, S_0 = 0.5, \omega = 20, Sc = 0.22, \alpha = \frac{\pi}{4}, Re = 10$.*

ϕ	H	G_m	S	R	G_r	λ	$-Cf$	Enhancement(%)
0.05	1.5	5	2	0.5	5	1.4	0.203108111	
0.0525	1.5	5	2	0.5	5	1.4	0.201751152	-0.668
0.055	1.5	5	2	0.5	5	1.4	0.200389459	-0.675
0.0575	1.5	5	2	0.5	5	1.4	0.199023038	-0.682
0.06	1.5	5	2	0.5	5	1.4	0.197651889	-0.689
Slope							-0.54562232	
0.04	1	5	2	0.5	5	1.4	0.189942907	
0.04	1.125	5	2	0.5	5	1.4	0.194262629	2.274
0.04	1.25	5	2	0.5	5	1.4	0.198388724	2.124
0.04	1.375	5	2	0.5	5	1.4	0.202275413	1.959
0.04	1.5	5	2	0.5	5	1.4	0.20589929	1.792
Slope							0.03194044	
0.04	1.5	3	2	0.5	5	1.4	0.177751404	
0.04	1.5	3.5	2	0.5	5	1.4	0.184788376	3.959
0.04	1.5	4	2	0.5	5	1.4	0.191825347	3.808
0.04	1.5	4.5	2	0.5	5	1.4	0.198862319	3.668
0.04	1.5	5	2	0.5	5	1.4	0.20589929	3.539
Slope							0.014073943	
0.04	1.5	5	2.5	0.5	5	1.4	0.214495149	
0.04	1.5	5	2.625	0.5	5	1.4	0.216330949	0.856
0.04	1.5	5	2.75	0.5	5	1.4	0.218190236	0.859
0.04	1.5	5	2.875	0.5	5	1.4	0.220073412	0.863
0.04	1.5	5	3	0.5	5	1.4	0.221980887	0.867
Slope							0.014971151	
0.04	1.5	5	2	0.1	5	1.4	0.22571289	
0.04	1.5	5	2	0.125	5	1.4	0.225624356	-0.039
0.04	1.5	5	2	0.15	5	1.4	0.225516217	-0.048
0.04	1.5	5	2	0.175	5	1.4	0.225388517	-0.057
0.04	1.5	5	2	0.2	5	1.4	0.225241303	-0.065
Slope							-0.004716052	
0.04	1.5	5	2	0.5	3	1.4	0.126386072	
0.04	1.5	5	2	0.5	3.5	1.4	0.15109988	19.554
0.04	1.5	5	2	0.5	4	1.4	0.175813688	16.356
0.04	1.5	5	2	0.5	4.5	1.4	0.200527496	14.057
0.04	1.5	5	2	0.5	5	1.4	0.225241303	12.324
Slope							0.049427616	
0.04	1.5	5	2	0.5	5	1	0.061783952	
0.04	1.5	5	2	0.5	5	1.1	0.092068285	49.017
0.04	1.5	5	2	0.5	5	1.2	0.126548023	37.45
0.04	1.5	5	2	0.5	5	1.3	0.165346706	30.659
0.04	1.5	5	2	0.5	5	1.4	0.208586679	26.151
Slope							0.366883875	

Table 2.5: *The Nusselt number of Fe_3O_4-water nanofluid when $t = \frac{\pi}{4}, Pr = 6.07,\ G_r = 5,\quad G_m = 5,\quad K_r = 1.5,\quad K_1 = 0.7,\ M = 3.5, H = 1.5,\ S_0 = 0.5,\ \omega = 20,\quad Sc = 0.22, \alpha = \frac{\pi}{4},\ Re = 10.$*

ϕ	S	R	λ	Nu	Enhancement(%)
0.05	2	0.5	1.4	10.47453	
0.0525	2	0.5	1.4	10.46772	-0.065
0.055	2	0.5	1.4	10.4609	-0.065
0.0575	2	0.5	1.4	10.45407	-0.065
0.06	2	0.5	1.4	10.44724	-0.065
Slope				-2.72878	
0.04	2.8	0.5	1.4	11.1924	
0.04	2.85	0.5	1.4	11.24113	0.435
0.04	2.9	0.5	1.4	11.29012	0.436
0.04	2.95	0.5	1.4	11.33938	0.436
0.04	3	0.5	1.4	11.3889	0.437
Slope				0.982513	
0.04	2	0.1	1.4	11.6304	
0.04	2	0.125	1.4	11.62467	-0.049
0.04	2	0.15	1.4	11.61767	-0.06
0.04	2	0.175	1.4	11.6094	-0.071
0.04	2	0.2	1.4	11.59987	-0.082
Slope				-0.30535	
0.04	2	0.5	1	8.354338	
0.04	2	0.5	1.1	9.018292	7.947
0.04	2	0.5	1.2	9.673948	7.27
0.04	2	0.5	1.3	10.32214	6.7
0.04	2	0.5	1.4	10.96381	6.216
Slope				6.5228	

2.4.1 Statistical analysis

The impact of different parameters on Cf, Nu and Sh (z = 1) are established using r_c (Correlation coefficient) and PE (Probable error) described in the tables 2.7 to 2.9. The sign of r_c determines the nature of relationship and the magnitude of r_c indicates the intensity of relationship (Mackolil & Mahanthesh, 2019). The significance in the precision of correlation coefficient is verified using PE of r_c and the correlation is said to be significant if $|r_c| > 6.|PE|$ (Fisher et al., 1921) Probable error is calculated using the formula, PE = $(\ \frac{1-{r_c}^2}{\sqrt{\tilde{n}}})$ 0.6745; where $\tilde{n}$ is the number of observations. From Table 2.7, it is observed that Cf has high positive correlation with ϕ and R and high negative correlation with H, G_m, S, G_r and λ. All the values

p

Table 2.6: *The Sherwood number of Fe_3O_4-water nanofluid when $Pr = 6.07, G_r = 5,\ G_m = 5,\ K_1 = 0.7,\ M = 3.5,\ H = 1.5,\ S = 2, Sc = 0.22,\ \alpha = \frac{\pi}{4}$.*

ϕ	R	S_0	λ	ω	t	K_r	Sh	Enhancement(%)
0.05	0.5	0.5	1.4	20	0.785	1	0.21135492	
0.0525	0.5	0.5	1.4	20	0.785	1	0.21771996	3.012
0.055	0.5	0.5	1.4	20	0.785	1	0.22403398	2.9
0.0575	0.5	0.5	1.4	20	0.785	1	0.23029753	2.796
0.06	0.5	0.5	1.4	20	0.785	1	0.23651114	2.698
Slope							2.51559988	
0.04	0.1	0.5	1.4	20	0.785	1	0.12563614	
0.04	0.125	0.5	1.4	20	0.785	1	0.12617555	0.429
0.04	0.15	0.5	1.4	20	0.785	1	0.12683434	0.522
0.04	0.175	0.5	1.4	20	0.785	1	0.12761224	0.613
0.04	0.2	0.5	1.4	20	0.785	1	0.1285089	0.703
Slope							0.02872886	
0.04	0.5	0.1	1.4	20	0.785	1	0.86984265	
0.04	0.5	0.2	1.4	20	0.785	1	0.68450921	-21.307
0.04	0.5	0.3	1.4	20	0.785	1	0.49917578	-27.075
0.04	0.5	0.4	1.4	20	0.785	1	0.31384234	-37.128
0.04	0.5	0.5	1.4	20	0.785	1	0.1285089	-59.053
Slope							-1.85333436	
0.04	0.5	0.5	1	20	0.785	1	0.38038438	
0.04	0.5	0.5	1.1	20	0.785	1	0.31760915	-16.503
0.04	0.5	0.5	1.2	20	0.785	1	0.25475175	-19.791
0.04	0.5	0.5	1.3	20	0.785	1	0.19174312	-24.733
0.04	0.5	0.5	1.4	20	0.785	1	0.1285089	-32.979
Slope							-0.62961697	
0.04	0.5	0.5	1.4	25	0.785	1	0.1281293	
0.04	0.5	0.5	1.4	25.25	0.785	1	0.12810759	-0.017
0.04	0.5	0.5	1.4	25.5	0.785	1	0.12808535	-0.017
0.04	0.5	0.5	1.4	25.75	0.785	1	0.12806256	-0.018
0.04	0.5	0.5	1.4	26	0.785	1	0.12803922	-0.018
Slope							-9.01E-05	
0.04	0.5	0.5	1.4	20	1	1	0.12798591	
0.04	0.5	0.5	1.4	20	1.125	1	0.12774596	-0.187
0.04	0.5	0.5	1.4	20	1.25	1	0.12735648	-0.305
0.04	0.5	0.5	1.4	20	1.375	1	0.12682355	-0.418
0.04	0.5	0.5	1.4	20	1.5	1	0.12615547	-0.527
Slope							-0.00366663	
0.04	0.5	0.5	1.4	20	0.785	0.5	0.1888454	
0.04	0.5	0.5	1.4	20	0.785	0.625	0.18065067	-4.339
0.04	0.5	0.5	1.4	20	0.785	0.75	0.17256179	-4.478
0.04	0.5	0.5	1.4	20	0.785	0.875	0.16457699	-4.627
0.04	0.5	0.5	1.4	20	0.785	1	0.15669457	-4.79
Slope							-0.06430027	

p

Table 2.7: *Correlation coefficient (r_c), Probable error (PE) and $|\frac{r_c}{PE}|$ values of Cf with respect to the parameters ϕ, H, G_m , S, R, G_r and λ*

Parameter	r_c	PE	$\lvert\frac{r_c}{PE}\rvert$
ϕ	0.999997896	1.27E-06	787896.2218
H	-0.99940294	0.000360093	2775.399238
G_m	-1	0	Inf
S	-0.999971478	1.72E-05	58114.63519
R	0.995217965	0.002878061	345.7945854
G_r	-1	1.34E-16	7.47E+15
λ	-0.997583808	0.001455906	685.1977823

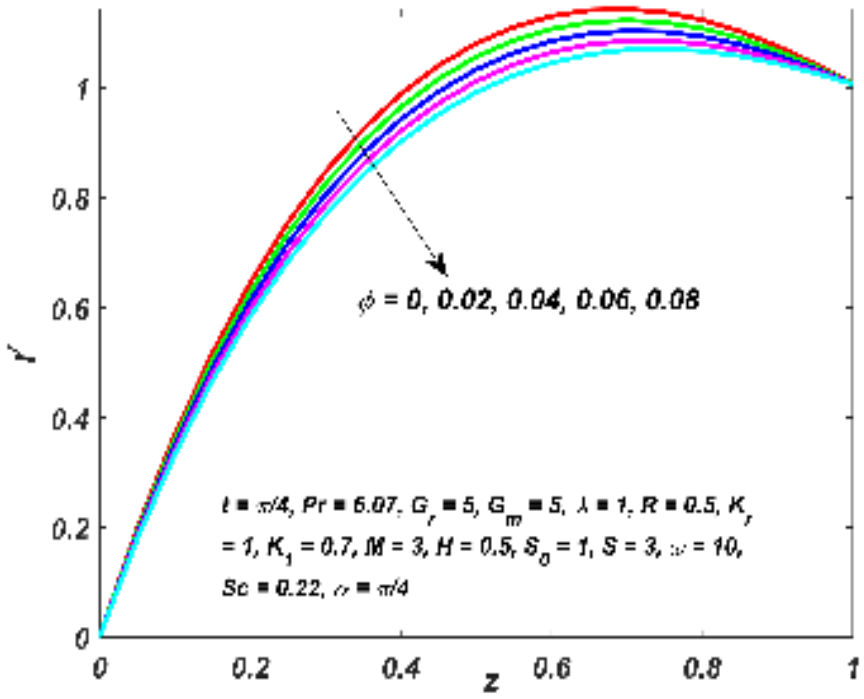

Figure 2.2: *Variations in Velocity l' with ϕ*

of $\left|\frac{r_c}{PE}\right|$ for Cf are greater than 6 meaning that the parameters described in the table are significant. Table 2.8 proposes that Nu is highly negatively correlated with ϕ and R and positively correlated with S and λ. From table 2.9, it can be inferred that Sh is highly positively correlated with ϕ and R and highly negatively correlated with S_0, λ, ω, t and K_r .

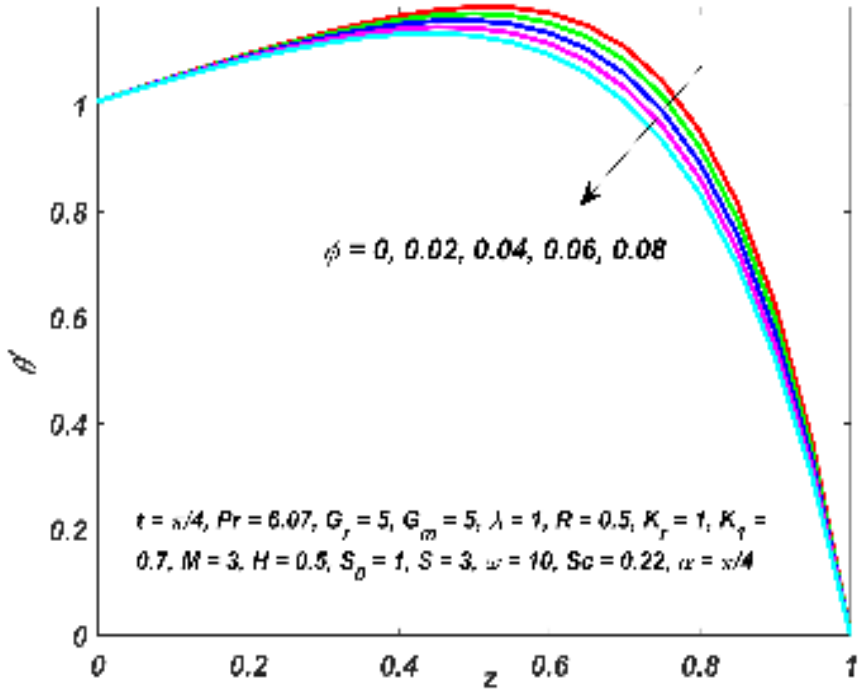

Figure 2.3: *Variations in temperature θ' with ϕ*

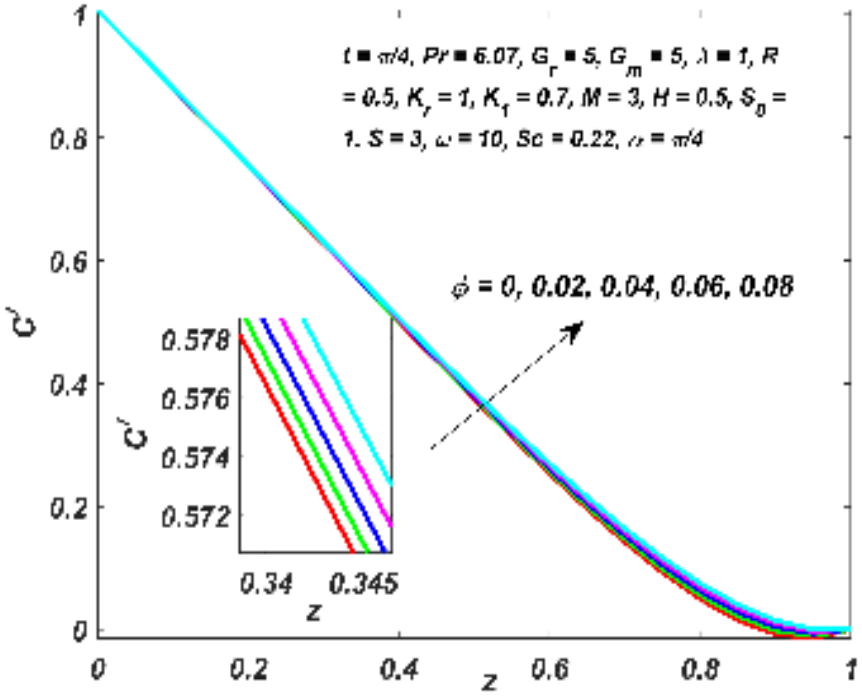

Figure 2.4: *Variations in concentration C' with ϕ*

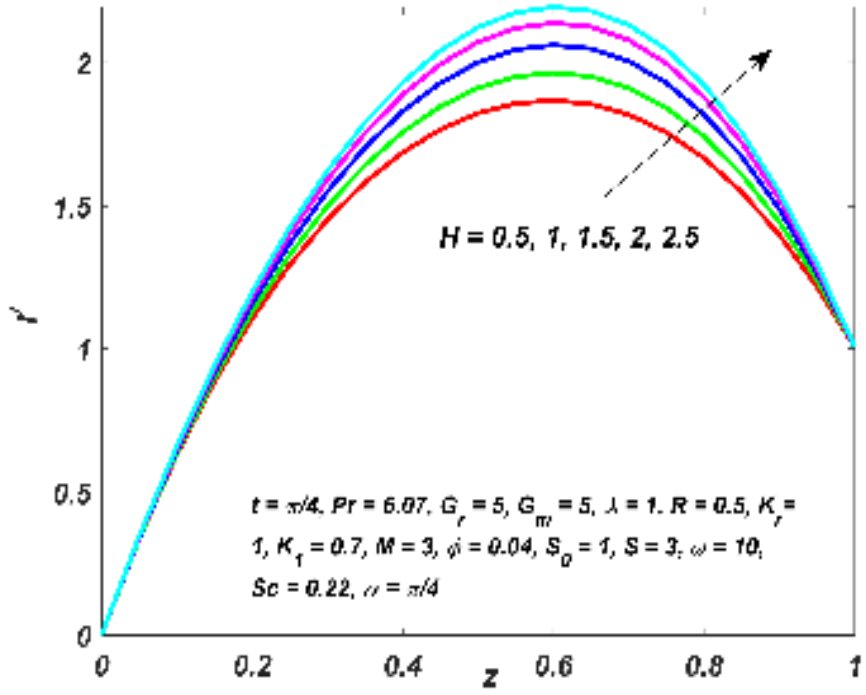

Figure 2.5: *Variations in velocity l' with H*

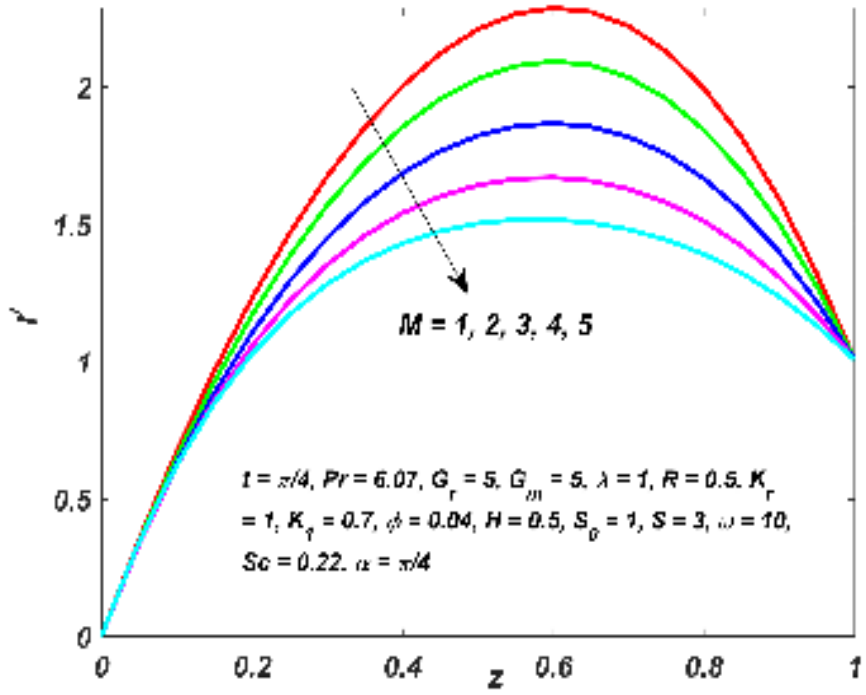

Figure 2.6: *Variations in velocity l' with M*

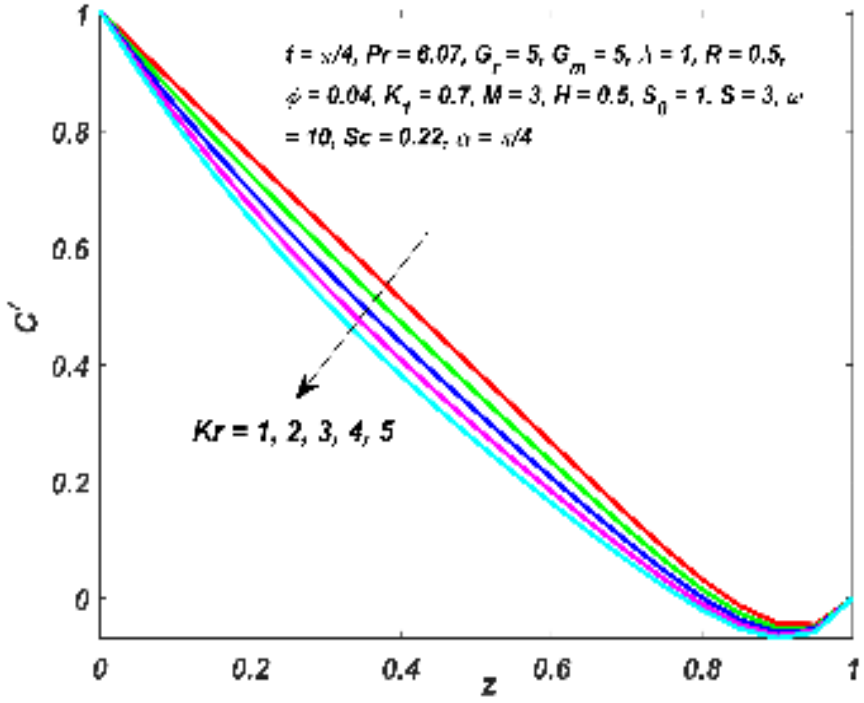

Figure 2.7: *Variations in concentration* C' *with* $K_r > 0$

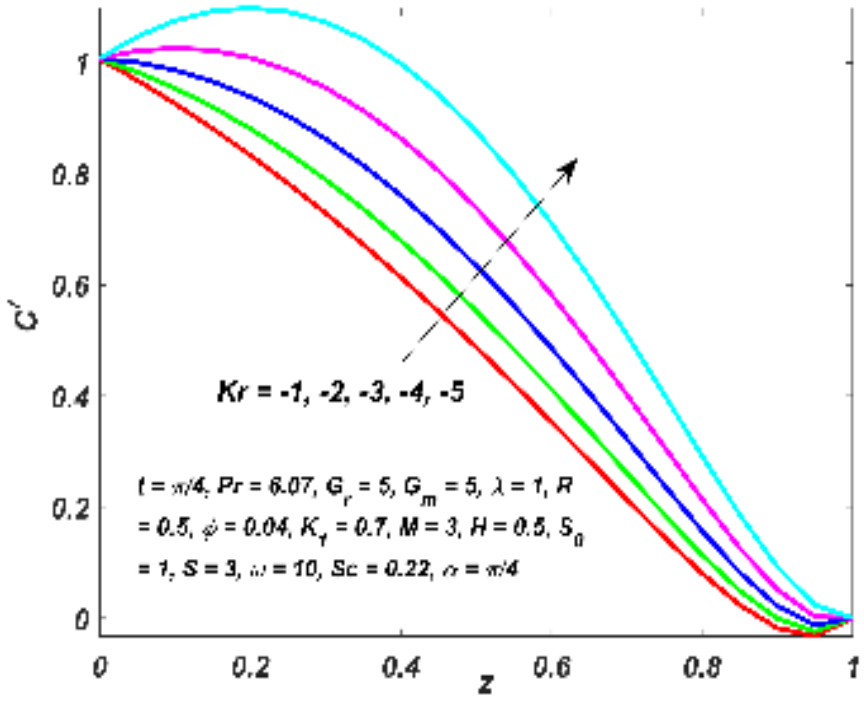

Figure 2.8: *Variations in concentration* C' *with* $(K_r < 0)$

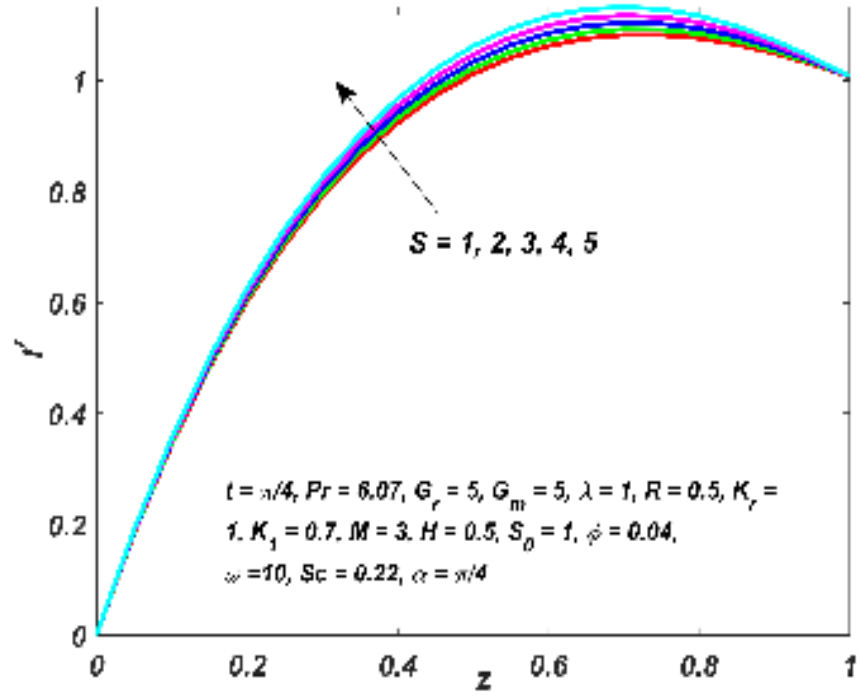

Figure 2.9: *Variations in velocity l' with S*

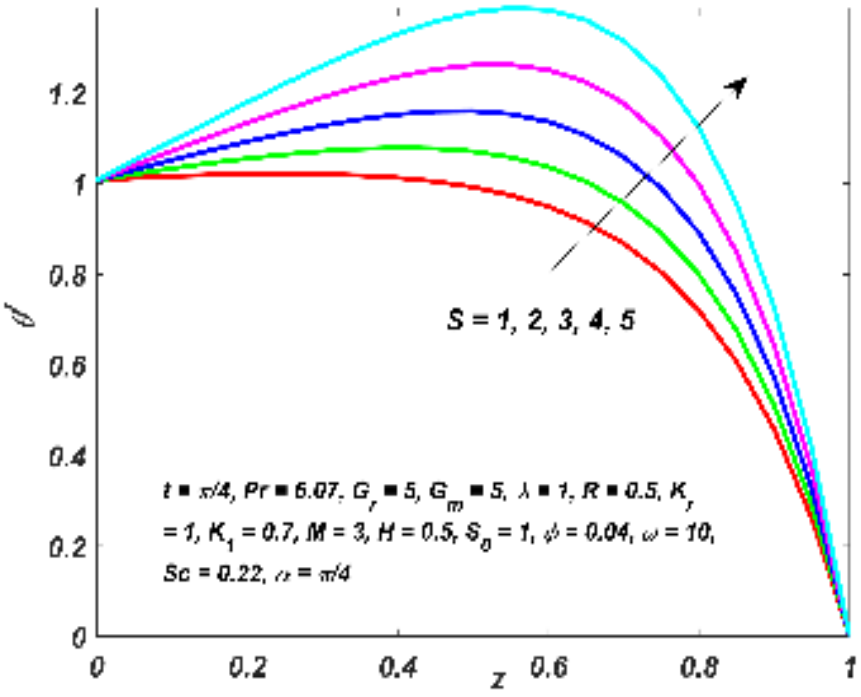

Figure 2.10: *Variations in temperature$\theta'$with S*

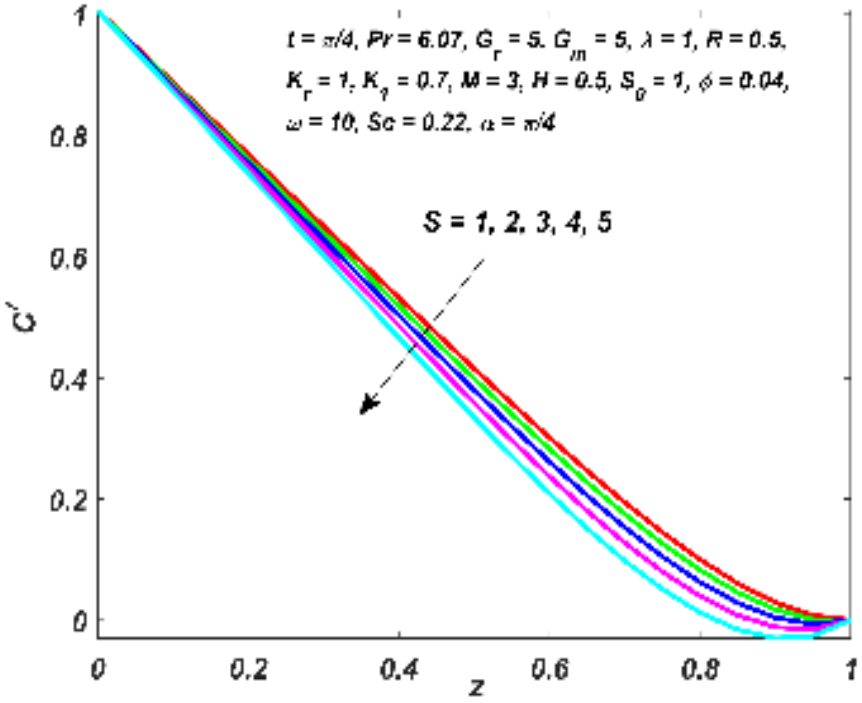

Figure 2.11: *Variations in concentration C' with S*

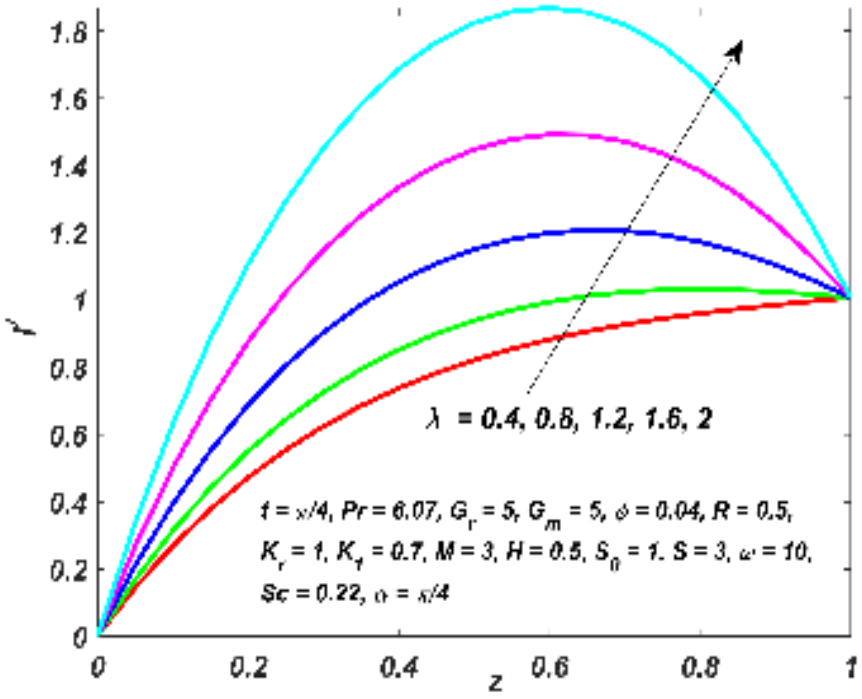

Figure 2.12: *Variations in velocity l' with λ*

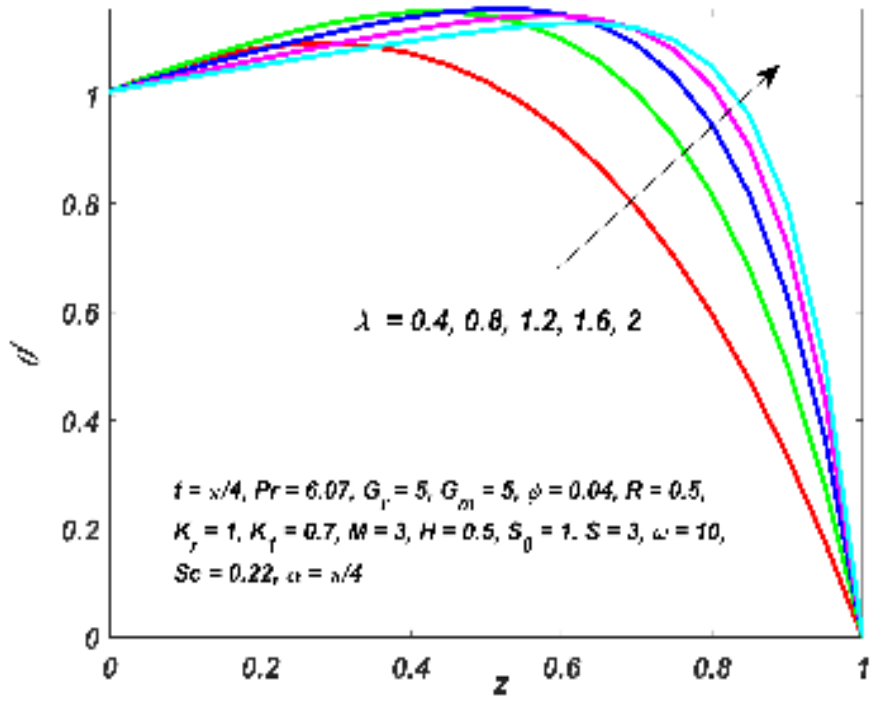

Figure 2.13: *Variations in temperature θ' with λ*

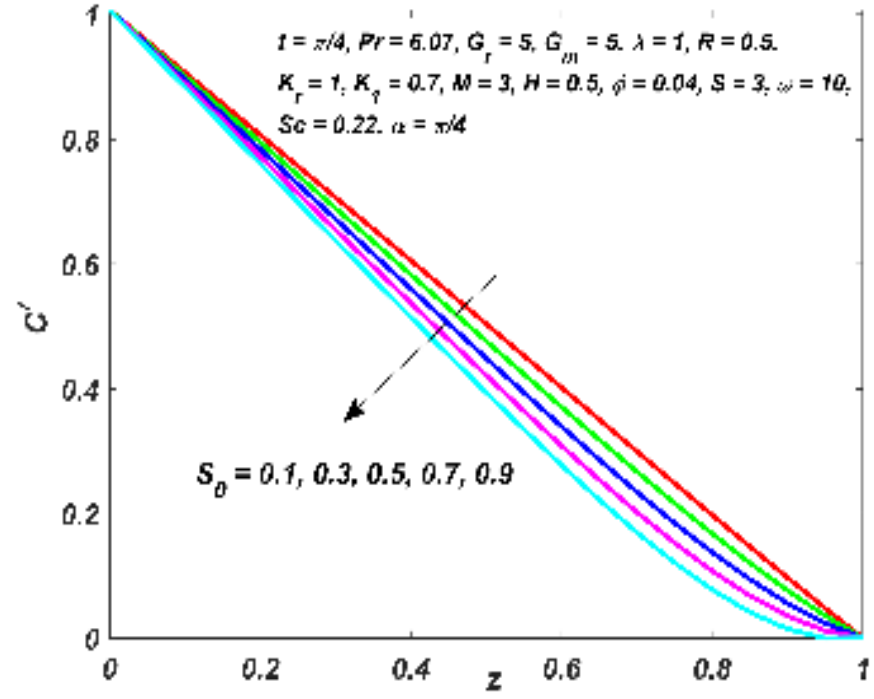

Figure 2.14: *Variations in concentration C' with S_0*

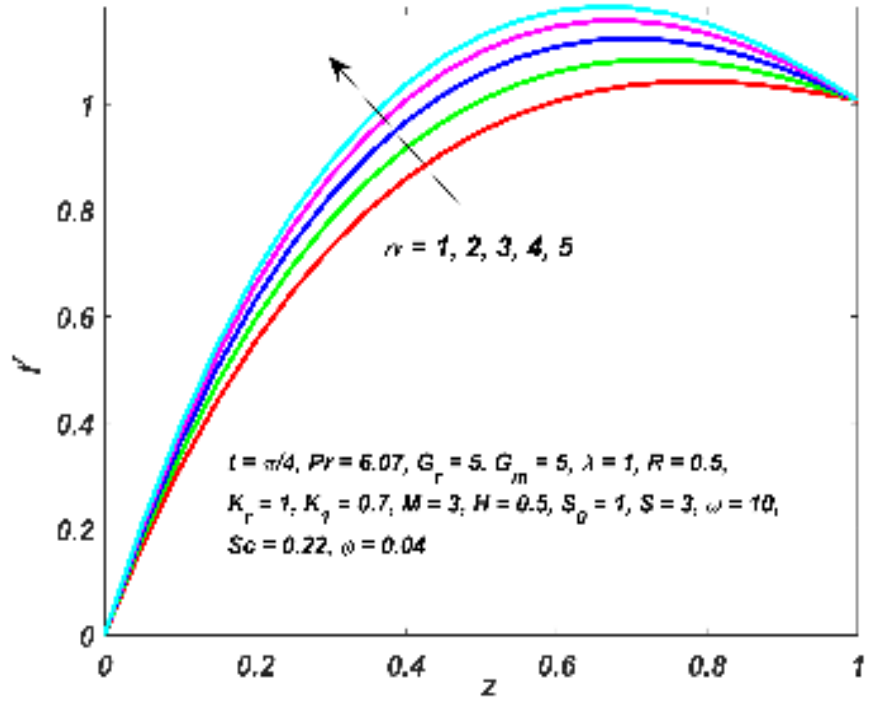

Figure 2.15: *Variations in velocity l' with α*

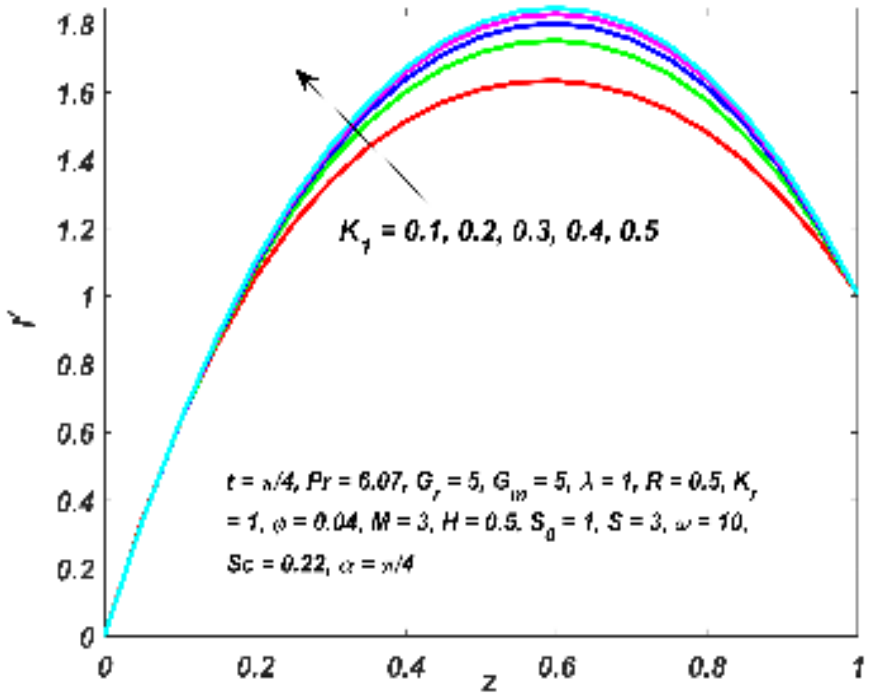

Figure 2.16: *Variations in velocity l' with K_1*

Table 2.8: *Correlation coefficient (r_c), Probable error (PE) and $|\frac{r_c}{PE}|$ values of Nu with respect to the parameters ϕ, S, R and λ*

parameter	r_c	PE	$\lvert\frac{r_c}{PE}\rvert$.
ϕ	-0.999999812	1.13E-07	8835395.319
S	0.999994883	3.09E-06	323962.1929
R	-0.995220189	0.002876726	345.9558435
λ	0.999977238	1.37E-05	72822.19318

Table 2.9: *Correlation coefficient (r_c), Probable error (PE) and $|\frac{r_c}{PE}|$ values of Sh with respect to the parameters $\phi, R, S_0, \lambda, \omega, t$ and K_r*

parameter	r_c	PE	$\left\lvert\frac{r_c}{PE}\right\rvert$
ϕ	0.999988727	6.80E-06	147044.3608
R	0.995223125	0.002874963	346.1690028
S_0	-1	0	Inf
λ	-0.999998944	6.37E-07	1569871.63
ω	-0.999897527	6.18E-05	16174.89232
t	-0.983424825	0.009916783	99.16772636
K_r	-0.999970646	1.77E-05	56468.14162

2.4.2 Regression analysis

Regression analysis is a statistical modelling technique used to establish a relationship between a dependent and one or more independent variables. Tables 2.7 to 2.9 reflect the nature of relationship with single variable whereas in regression analysis the quantity of relationship is obtained with more than one independent variable. $Cf,\ Nu$ and Sh are estimated using multiple linear regression models given by the form:

$$Cf_{est} = c + b_\phi\ \phi + b_H H + b_{G_m} G_m + b_S\ S + b_R\ R + b_{Gr} G_r + b_\lambda\ \lambda \tag{2.4.1}$$

$$Nu_{est} = c + b_\phi\ \phi + b_S\ S + b_R R + b_\lambda\ \lambda \tag{2.4.2}$$

$$Sh_{est} = c + b_\phi\ \phi + b_R\ R + b_{S_0} S_0 + b_\lambda \lambda + b_\omega\ \omega + b_t\ t + b_{K_r} K_r \tag{2.4.3}$$

where $c, b_\phi, b_H, b_{G_m}\ , b_S, b_R, b_{G_r}, b_\lambda, b_{S_0}, b_\omega, b_t$ and b_{K_r} are the estimated regression coefficients. These values are estimated from the table (2.4-2.6) values using MATLAB

software. It can be noted from tables 2.10-2.12 that all Sig. value < 0.05 (p Value) proving that the calculated regression coefficients are significant. From tables 2.10 to 2.12 it is observed that the R-squared values are approximately equal to 1 and also error is negligibly small (close to 0) meaning that the test is effective. The estimated Cf, Nu and Sh are:

Table 2.10: *Linear regression model for Cf, with Number of observations :35, Error degrees of freedom:27, Root mean square error :0.00461, $\mathcal{R}$-squared:0.989, Adjusted $\mathcal{R}$-Squared 0.986, F-statistic vs. constant model:332, p-value =1.7e-24*

Variables	Estimate	SE	tStat	p Value
Intercept	0.652031	0.027974	23.31551	2.02E-19
ϕ	0.654027	0.171889	3.804932	0.00074
H	-0.043	0.008129	-5.28944	1.40E-05
G_m	-0.017	0.002032	-8.36414	5.65E-09
S	-0.0108	0.003438	-3.14246	0.004041
R	0.043069	0.007597	5.669406	5.08E-06
G_r	-0.03946	0.002032	-1.4154	2.16E-17
λ	-0.38702	0.010161	-38.0881	5.25E-25

Table 2.11: *Linear regression model for Nu with number of observations :20, Error degrees of freedom:15, mean square error :0.0713, $\mathcal{R}$-squared: 0.995, Adjusted $\mathcal{R}$- Squared 0.994, F-statistic vs. constant model:773, p-value =3.59e-17*

Variables	Estimate	SE	tStat	p Value
Intercept	3.350136	0.217599	15.39591	1.34E-10
ϕ	-28.7968	3.787674	-7.60277	1.60E-06
S	0.42104	0.065763	6.402399	1.19E-05
R	-1.98807	0.168527	-11.7967	5.46E-09
λ	6.334471	0.212077	29.86876	8.87E-15

$$Cf_{est} = 0.652231 + 0.654027\ \phi - 0.043\ H - 0.017\ G_m - 0.0108\ S + 0.043069\ R - 0.03946\ G_r - 0.38702\ \lambda \tag{2.4.4}$$

$$Nu_{est} = 3.350136 - 28.7968\ \phi + 0.42104\ S - 1.98807\ R + 6.334471\ \lambda \tag{2.4.5}$$

$$Sh_{est} = 1.812674 + 5.495754\ \phi + 0.034541\ R - 1.818151\ S_0 - 0.594991\lambda \\ -0.001988\ \omega - 0.022729\ t - 0.111039\ K_r \tag{2.4.6}$$

It is understood from the regression equations that H, G_m, S, G_r and λ have a negative impact on Cf whereas R and ϕ has a positive impact on Cf. The mounting values of R and ϕ creates a significant increase in the values of Cf while it reverses in the case of negatively impacted parameters.These results coincide with the results described in table 2.7. Enhancing the value of ϕ and R diminishes the value of Nu while an increase in S and λ increases the value of Nu. These results are in perfect synchronization with the observations in Table 2.8. Similarly, from the regression equation for Sh, it is understood that ϕ and R have a positive impact on Sh whereas S_0, λ, ω, t and K_r have a negative impact on Sh. This is in agreement with the findings in Table 2.9. Figures 2.17 -2.19 illustrates the accuracy of the regression model for the chosen sample. A commendable agreement is noted between the numerically calculated values and regression values.

Table 2.12: *Linear regression model for Sh, Number of observations :35, Error degrees of freedom:27, Root mean square error :0.00753, $\mathcal{R}$-squared:0.998, Adjusted $\mathcal{R}$-Squared 0.998, F-statistic vs. constant model:2.31e+03, p-value =8.37e-36*

Variables	Estimate	SE	tStat	p value
Intercept	1.812674817	0.02908886	62.31508568	1.03E-30
ϕ	5.495754491	0.292700432	18.77603823	5.02E-17
R	0.034541513	0.012949556	2.667389769	0.012762683
S_0	-1.818151624	0.017165431	-105.9193681	6.57E-37
λ	-0.594991434	0.017165431	-34.66218983	6.36E-24
ω	-0.001988324	0.000827683	-2.402277412	0.023439152
t	-0.022729364	0.00891019	-2.550940334	0.01672498
K_r	-0.111039183	0.013732345	-8.08595936	1.09E-08

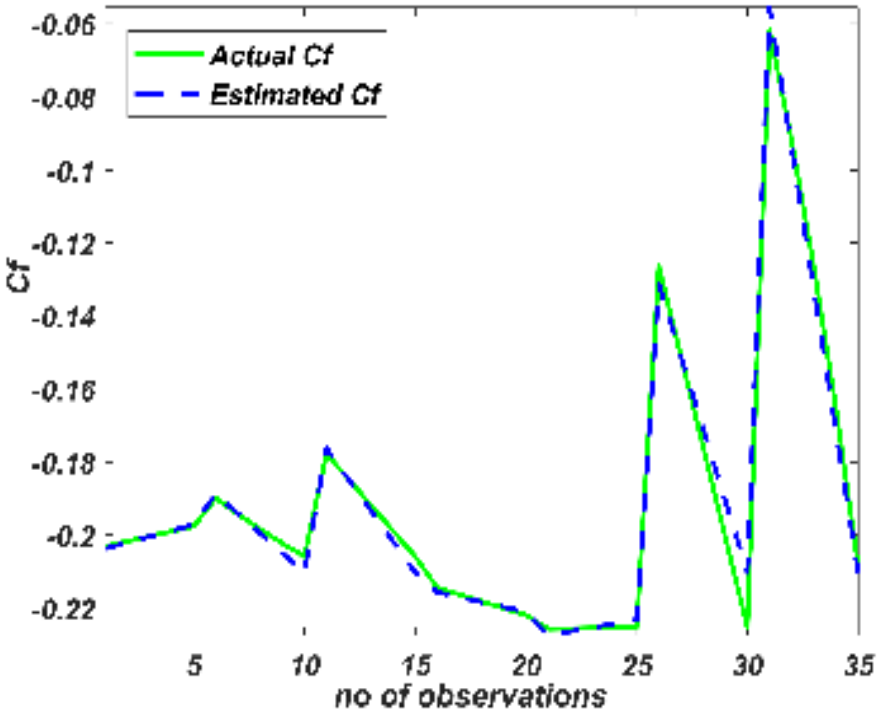

Figure 2.17: *Actual and estimated values of* Cf

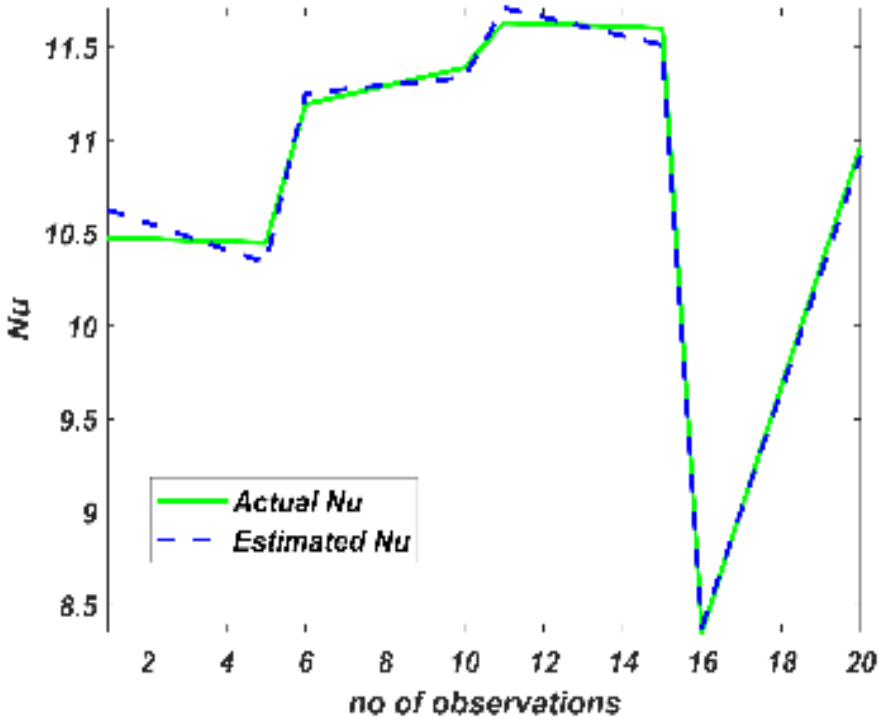

Figure 2.18: *Actual and estimated values of* Nu

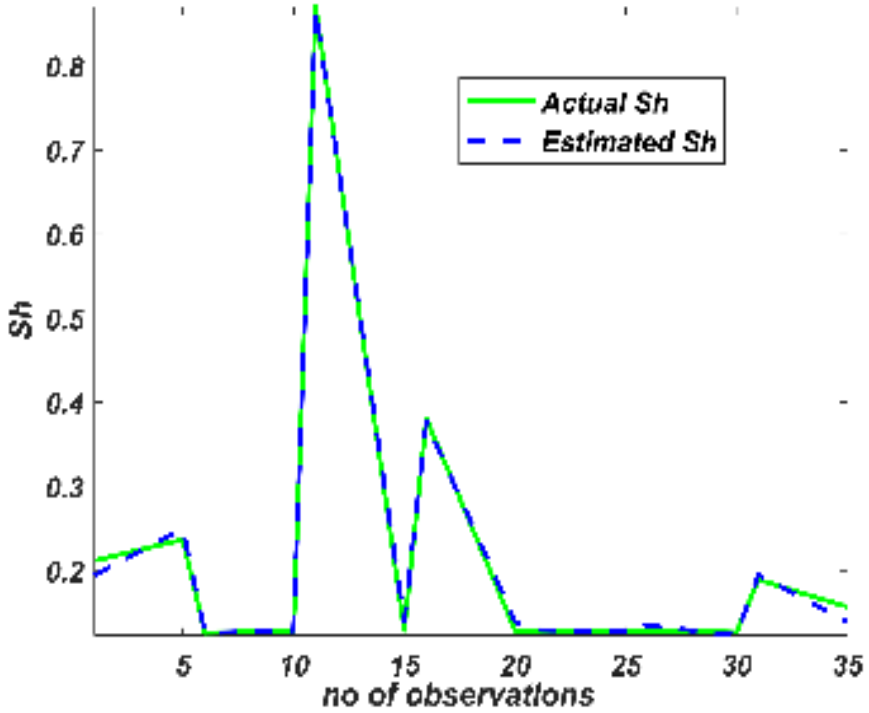

Figure 2.19: *Actual and estimated values of Sh*

2.5 Conclusions

The influence of heat source and hall current on magneto-hydrodynamic ferro-nanoflow in an inclined porous channel with radiation and chemical reaction has been theoretically analysed. The major conclusions drawn from the current analysis are given below:

- Hall current and injection/suction parameter play a crucial role in amplifying the velocity profile.
- The temperature and velocity profiles are directly proportional to the heat source parameter, S.
- Angle of inclination, α has a constructive effect on the velocity profiles.
- The volume fraction of the nanoparticles, ϕ enhances the concentration profiles but reduces the temperature and velocity profiles.
- Increase in Hartmann number accounts for a reduction in velocity profile.
- The Soret effect has a destructive impact on concentration profiles.

- Heat source and hall current has a negative impact on skin friction.

- An increase of 0.982513 per unit S (heat source) is noted due to the impact of heat source on Nusselt number.

- Soret number has a negative impact (a decrease of 1.853334359 per unit S_o) on Sherwood number.

Our future aim is to extend the present study by incorporating viscous dissipation, Joule heating and entropy generations which are decisive in heat and mass transfer rates.

2.6 Appendix

$$\eta_1 = \frac{\phi_4\lambda + \sqrt{(\phi_4\lambda)^2 - 4\lambda_n \frac{(-R^2+S)}{(P_r)^2}}}{2\left(\frac{\lambda_n}{P_r}\right)} \tag{2.6.1}$$

$$\eta_2 = \frac{\phi_4\lambda - \sqrt{(\phi_4\lambda)^2 - 4\lambda_n \frac{(-R^2+S)}{(P_r)^2}}}{2\left(\frac{\lambda_n}{P_r}\right)} \tag{2.6.2}$$

$$\eta_3 = \frac{\phi_4\lambda + \sqrt{(\phi_4\lambda)^2 - 4\frac{\lambda_n}{P_r}\left(\frac{S}{P_r} - \frac{R^2}{P_r} - \omega i\phi_4\right)}}{2\left(\frac{\lambda_n}{P_r}\right)} \tag{2.6.3}$$

$$\eta_4 = \frac{\phi_4\lambda - \sqrt{(\phi_4\lambda)^2 - 4\frac{\lambda_n}{P_r}\left(\frac{S}{P_r} - \frac{R^2}{P_r} - \omega i\phi_4\right)}}{2\left(\frac{\lambda_n}{P_r}\right)} \tag{2.6.4}$$

$$\eta_5 = \frac{\phi_4\lambda + \sqrt{(\phi_4\lambda)^2 - 4\frac{\lambda_n}{P_r}\left(\frac{S}{P_r} - \frac{R^2}{P_r} + \omega i\phi_4\right)}}{2\left(\frac{\lambda_n}{P_r}\right)} \tag{2.6.5}$$

$$\eta_6 = \frac{\phi_4\lambda - \sqrt{(\phi_4\lambda)^2 - 4\frac{\lambda_n}{P_r}\left(\frac{S}{P_r} - \frac{R^2}{P_r} + \omega i\phi_4\right)}}{2\left(\frac{\lambda_n}{P_r}\right)} \tag{2.6.6}$$

$$q_1 = \frac{\lambda + \sqrt{\lambda^2 + 4K_r\frac{\lambda^2}{S_c}}}{\frac{2}{S_c}} \tag{2.6.7}$$

$$q_2 = \frac{\lambda - \sqrt{\lambda^2 + 4K_r\frac{\lambda^2}{S_c}}}{\frac{2}{S_c}} \tag{2.6.8}$$

$$q_3 = \frac{\lambda + \sqrt{\lambda^2 + \frac{4}{S_c}\left(K_r\lambda^2 + \omega i\right)}}{\frac{2}{S_c}} \tag{2.6.9}$$

$$q_4 = \frac{\lambda - \sqrt{\lambda^2 + \frac{4}{S_c}\left(K_r\lambda^2 + \omega i\right)}}{\frac{2}{S_c}} \tag{2.6.10}$$

$$q_5 = \frac{\lambda + \sqrt{\lambda^2 + \frac{4}{S_c}\left(K_r\lambda^2 - \omega i\right)}}{\frac{2}{S_c}} \tag{2.6.11}$$

$$q_6 = \frac{\lambda - \sqrt{\lambda^2 + \frac{4}{S_c}\left(K_r\lambda^2 - \omega i\right)}}{\frac{2}{S_c}} \tag{2.6.12}$$

$$\chi_1 = \frac{\phi_1\lambda + \sqrt{\left(\phi_1\lambda\right)^2 + 4\phi_2 p'}}{2\phi_2} \tag{2.6.13}$$

$$\chi_2 = \frac{\phi_1\lambda - \sqrt{\left(\phi_1\lambda\right)^2 + 4\phi_2 p'}}{2\phi_2} \tag{2.6.14}$$

$$\chi_3 = \frac{\phi_1\lambda + \sqrt{\left(\phi_1\lambda\right)^2 + 4\phi_2 q'}}{2\phi_2} \tag{2.6.15}$$

$$\chi_4 = \frac{\phi_1\lambda - \sqrt{\left(\phi_1\lambda\right)^2 + 4\phi_2 q'}}{2\phi_2} \tag{2.6.16}$$

$$\chi_5 = \frac{\phi_1\lambda + \sqrt{\left(\phi_1\lambda\right)^2 + 4\phi_2 r'}}{2\phi_2} \tag{2.6.17}$$

$$\chi_6 = \frac{\phi_1\lambda - \sqrt{\left(\phi_1\lambda\right)^2 + 4\phi_2 r'}}{2\phi_2} \tag{2.6.18}$$

$$A_{11} = \frac{-S_0(\eta_1)^2 m_1}{\frac{1}{S_c}(\eta_1)^2 - \lambda\eta_1 - K_r\lambda^2} \tag{2.6.19}$$

$$A_{12} = \frac{-S_0(\eta_2)^2 m_2}{\frac{1}{S_c}(\eta_2)^2 - \lambda\eta_2 - K_r\lambda^2} \tag{2.6.20}$$

$$A_{21} = \frac{-S_0(\eta_3)^2 m_3}{\frac{1}{S_c}(\eta_3)^2 - \lambda\eta_3 - \left(K_r\lambda^2 + \omega i\right)} \tag{2.6.21}$$

$$A_{22} = \frac{-S_0(\eta_4)^2 m_4}{\frac{1}{S_c}(\eta_4)^2 - \lambda\eta_4 - (K_r\lambda^2 + \omega i)} \tag{2.6.22}$$

$$A_{31} = \frac{-S_0(\eta_5)^2 m_5}{\frac{1}{S_c}(\eta_5)^2 - \lambda\eta_5 + (-K_r\lambda^2 + \omega i)} \tag{2.6.23}$$

$$A_{32} = \frac{-S_0(\eta_6)^2 m_6}{\frac{1}{S_c}(\eta_6)^2 - \lambda\eta_6 + (-K_r\lambda^2 + \omega i)} \tag{2.6.24}$$

$$D_{11} = 1 \tag{2.6.25}$$

$$D_{12} = \frac{-\phi_3 G_r(\lambda)^2 m_1 sin\alpha}{\phi_2(\eta_1)^2 - \phi_1\lambda\eta_1 - p'} \tag{2.6.26}$$

$$D_{13} = \frac{-\phi_3 G_r(\lambda)^2 m_2 sin\alpha}{\phi_2(\eta_2)^2 - \phi_1\lambda\eta_2 - p'} \tag{2.6.27}$$

$$D_{14} = \frac{-\phi_3 G_m(\lambda)^2 \zeta_1 sin\alpha}{\phi_2(q_1)^2 - \phi_1\lambda q_1 - p'} \tag{2.6.28}$$

$$D_{15} = \frac{-\phi_3 G_m(\lambda)^2 \zeta_2 sin\alpha}{\phi_2(q_2)^2 - \phi_1\lambda q_2 - p'} \tag{2.6.29}$$

$$D_{16} = \frac{-\phi_3 G_m(\lambda)^2 A_{11} sin\alpha}{\phi_2(\eta_1)^2 - \phi_1\lambda\eta_1 - p'} \tag{2.6.30}$$

$$D_{17} = \frac{-\phi_3 G_m(\lambda)^2 A_{12} sin\alpha}{\phi_2(\eta_2)^2 - \phi_1\lambda\eta_2 - p'} \tag{2.6.31}$$

$$D_{21} = 1 \tag{2.6.32}$$

$$D_{22} = \frac{-\phi_3 G_r(\lambda)^2 m_3 sin\alpha}{\phi_2(\eta_3)^2 - \phi_1\lambda\eta_3 - q'} \tag{2.6.33}$$

$$D_{23} = \frac{-\phi_3 G_r(\lambda)^2 m_4 sin\alpha}{\phi_2(\eta_4)^2 - \phi_1\lambda\eta_4 - q'} \tag{2.6.34}$$

$$D_{24} = \frac{-\phi_3 G_m(\lambda)^2 \zeta_3 sin\alpha}{\phi_2(q_3)^2 - \phi_1\lambda q_3 - q'} \tag{2.6.35}$$

$$D_{25} = \frac{-\phi_3 G_m(\lambda)^2 \zeta_4 sin\alpha}{\phi_2(q_4)^2 - \phi_1\lambda q_4 - q'} \tag{2.6.36}$$

$$D_{26} = \frac{-\phi_3 G_m(\lambda)^2 A_{21} sin\alpha}{\phi_2(\eta_3)^2 - \phi_1\lambda\eta_3 - q'} \tag{2.6.37}$$

$$D_{27} = \frac{-\phi_3 G_m(\lambda)^2 A_{22} sin\alpha}{\phi_2(\eta_4)^2 - \phi_1\lambda\eta_4 - q'} \tag{2.6.38}$$

$$D_{31} = 1 \tag{2.6.39}$$

$$D_{32} = \frac{-\phi_3 G_r(\lambda)^2 m_5 sin\alpha}{\phi_2(\eta_5)^2 - \phi_1\lambda\eta_5 - r'} \tag{2.6.40}$$

$$D_{33} = \frac{-\phi_3 G_r(\lambda)^2 m_6 sin\alpha}{\phi_2(\eta_6)^2 - \phi_1\lambda\eta_6 - r'} \tag{2.6.41}$$

$$D_{34} = \frac{-\phi_3 G_m(\lambda)^2 \zeta_5 sin\alpha}{\phi_2(q_5)^2 - \phi_1\lambda q_5 - r'} \tag{2.6.42}$$

$$D_{35} = \frac{-\phi_3 G_m(\lambda)^2 \zeta_6 sin\alpha}{\phi_2(q_6)^2 - \phi_1\lambda q_6 - r'} \tag{2.6.43}$$

$$D_{36} = \frac{-\phi_3 G_m(\lambda)^2 A_{31} sin\alpha}{\phi_2(\eta_5)^2 - \phi_1\lambda\eta_5 - r'} \tag{2.6.44}$$

$$D_{37} = \frac{-\phi_3 G_m(\lambda)^2 A_{32} sin\alpha}{\phi_2(\eta_6)^2 - \phi_1\lambda\eta_6 - r'} \tag{2.6.45}$$

$$m_1 = \frac{-\mathrm{e}^{(\eta_2)}}{e^{(\eta_1)} - \mathrm{e}^{(\eta_2)}} \tag{2.6.46}$$

$$m_2 = 1 - m_1 \tag{2.6.47}$$

$$m_3 = \frac{-\mathrm{e}^{(\eta_4)}}{e^{(\eta_3)} - \mathrm{e}^{(\eta_4)}} \tag{2.6.48}$$

$$m_4 = 1 - m_3 \tag{2.6.49}$$

$$m_5 = \frac{-e^{(\eta_6)}}{e^{(\eta_5)} - e^{(\eta_6)}} \tag{2.6.50}$$

$$m_6 = 1 - m_5 \tag{2.6.51}$$

$$\zeta_1 = \frac{e^{(q_2)} - A_{11}\left(e^{(q_2)} - e^{(\eta_1)}\right) + A_{12}\left(e^{(\eta_2)} - e^{(q_2)}\right)}{e^{(q_2)} - e^{(q_1)}} \tag{2.6.52}$$

$$\zeta_2 = 1 - \zeta_1 - A_{11} - A_{12} \tag{2.6.53}$$

$$\zeta_3 = \frac{e^{(q_4)} - A_{21}\left(e^{(q_4)} - e^{(\eta_3)}\right) + A_{22}\left(e^{(\eta_4)} - e^{(q_4)}\right)}{e^{(q_4)} - e^{(q_3)}} \tag{2.6.54}$$

$$\zeta_4 = 1 - \zeta_3 - A_{21} - A_{22} \tag{2.6.55}$$

$$\zeta_5 = \frac{e^{(q_6)} - A_{31}\left(e^{(q_6)} - e^{(\eta_5)}\right) + A_{32}\left(e^{(\eta_6)} - e^{(q_6)}\right)}{e^{(q_6)} - e^{(q_5)}} \tag{2.6.56}$$

$$\zeta_6 = 1 - \zeta_5 - A_{31} - A_{32} \tag{2.6.57}$$

$$h_1 = \frac{\begin{array}{r} -1 + \mathrm{D}_{11}(1 - \mathrm{e}^{(\chi_2)}) - D_{12}\left(e^{(\chi_2)} - e^{(\eta_1)}\right) \\ -D_{13}\left(e^{(\chi_2)} - e^{(\eta_2)}\right) + D_{14} \quad \left(e^{(q_1)} - e^{(\chi_2)}\right) + D_{15}\left(e^{(q_2)} - e^{(\chi_2)}\right) \\ +D_{16}\left(e^{(\eta_1)} - e^{(\chi_2)}\right) + D_{17}\left(e^{(\eta_2)} - e^{(\chi_2)}\right) \end{array}}{e^{(\chi_2)} - e^{(\chi_1)}} \tag{2.6.58}$$

$$h_2 = -h_1 - D_{11} - D_{12} - D_{13} - D_{14} - D_{15} - D_{16} - D_{17} \tag{2.6.59}$$

$$h_3 = \frac{\begin{array}{r} -1 + \mathrm{D}_{21}(1 - \mathrm{e}^{(\chi_4)}) - D_{22}\left(e^{(\chi_4)} - e^{(\eta_3)}\right) \\ -D_{23}\left(e^{(\chi_4)} - e^{(\eta_4)}\right) + D_{24}\left(e^{(q_3)} - e^{(\chi_4)}\right) + D_{25}\left(e^{(q_4)} - e^{(\chi_4)}\right) \\ +D_{26}\left(e^{(\eta_3)} - e^{(\chi_4)}\right) + D_{27}\left(e^{(\eta_4)} - e^{(\chi_4)}\right) \end{array}}{e^{(\chi_4)} - e^{(\chi_3)}} \tag{2.6.60}$$

$$h_4 = -h_3 - D_{21} - D_{22} - D_{23} - D_{24} - D_{25} - D_{26} - D_{27} \tag{2.6.61}$$

$$h_5 = \frac{\begin{array}{r} -1 + \mathrm{D}_{31}(1 - e^{(\chi_6)}) - D_{32}\left(e^{(\chi_6)} - e^{(\eta_5)}\right) \\ -D_{33}\left(e^{(\chi_6)} - e^{(\eta_6)}\right) + D_{34}\left(e^{(q_5)} - e^{(\chi_6)}\right) + D_{35}\left(e^{(q_6)} - e^{(\chi_6)}\right) \\ +D_{36}\left(e^{(\eta_5)} - e^{(\chi_6)}\right) + D_{37}\left(e^{(\eta_6)} - e^{(\chi_6)}\right) \end{array}}{e^{(\chi_6)} - e^{(\chi_5)}} \tag{2.6.62}$$

$$h_6 = -h_5 - D_{31} - D_{32} - D_{33} - D_{34} - D_{35} - D_{36} - D_{37} \tag{2.6.63}$$

$$p' = \frac{\phi_2}{K_1} + \frac{\phi_5 M^2}{1 + H^2} + \frac{\phi_5 M^2 i H}{1 + H^2} \tag{2.6.64}$$

$$q' = \frac{\phi_2}{K_1} + \frac{\phi_5 M^2}{1 + H^2} + \frac{\phi_5 M^2 i H}{1 + H^2} + \phi_1 \omega i \tag{2.6.65}$$

$$r' = \frac{\phi_2}{K_1} + \frac{\phi_5 M^2}{1 + H^2} + \frac{\phi_5 M^2 i H}{1 + H^2} - \phi_1 \omega i \tag{2.6.66}$$